

Article

Residual Stress-Driven Fatigue Life Optimization of Medical Welded Structures via Coupled Thermo-Mechanical Modeling

Claire Dubois ¹, Alexandre Lefèvre ¹ and Jean-Baptiste Martin ^{1,*}

¹ Department of Mechanical Engineering, École Polytechnique, Institut Polytechnique de Paris, Palaiseau, 91120, France

* Correspondence: Jean-Baptiste Martin, Department of Mechanical Engineering, École Polytechnique, Institut Polytechnique de Paris, Palaiseau, 91120, France

Abstract: The study investigates the influence of welding-induced residual stress on the fatigue life of medical welded structures using a coupled thermo-mechanical finite element framework. A moving double-ellipsoidal heat source model was employed to simulate the welding process of stainless steel medical components. Residual stress fields were extracted and mapped into a fatigue damage model based on stress-life (S-N) curves and rainflow cycle counting. Numerical simulations were conducted on 36 welding parameter combinations, covering heat inputs from 0.8 to 1.6 kJ/mm. The predicted peak tensile residual stress ranged from 210 to 385 MPa, leading to fatigue life variations of up to 3.4 times under identical external loading. The proposed optimization strategy achieved an average fatigue life improvement of 27.6% compared with baseline welding parameters, demonstrating its effectiveness for life enhancement design in medical devices.

Keywords: medical welded structures; residual stress; thermo-mechanical coupling; fatigue life prediction; welding optimization

1. Introduction

Welded joints are commonly used in medical devices and surgical instruments because they allow compact structural layouts, flexible geometric configurations, and efficient manufacturing. Typical applications include implantable components, minimally invasive surgical tools, and precision housings for diagnostic and therapeutic equipment. In such products, stainless steels and other biocompatible alloys are frequently employed to satisfy requirements on mechanical strength, corrosion resistance, and biological compatibility [1]. During long-term service, these welded structures are subjected to repeated mechanical loading arising from operational motion, vibration, and cyclic functional forces. Under these conditions, fatigue failure represents one of the primary damage mechanisms governing service life and structural reliability [2,3]. In contrast to static strength, fatigue behaviour in welded joints is strongly affected by local stress states and manufacturing-related factors. Among these factors, welding-induced residual stress has a direct influence on fatigue performance through its effect on the mean stress level under cyclic loading [4]. Recent studies on medical welded structures have demonstrated that welding process parameters and residual stress distributions can have a pronounced influence on fatigue life, highlighting the need for welding-process-level design optimisation in life-critical medical applications [5]. This sensitivity is particularly relevant for medical applications, where allowable failure probability is extremely small and reliability requirements are stringent.

Published: 21 February 2026



Copyright: © 2026 by the authors. Submitted for possible open access publication under the terms and conditions of the Creative Commons Attribution (CC BY) license (<https://creativecommons.org/licenses/by/4.0/>).

Residual stresses generated during welding originate from steep thermal gradients and constrained plastic deformation during heating and subsequent cooling. Tensile residual stresses are commonly observed near the weld toe and fusion zone, which also correspond to typical sites of fatigue crack initiation [6,7]. Under cyclic loading, these tensile stresses increase the effective stress ratio and accelerate crack nucleation as well as early-stage crack growth. In medical welded structures, the effect of residual stress is further amplified by thin-walled designs, tight dimensional tolerances, and strict requirements on geometric accuracy and functional stability [8]. These characteristics often limit the application of conventional post-weld stress relief methods, such as heat treatment or mechanical processing, due to the risk of distortion, microstructural modification, or loss of dimensional precision [9]. As a consequence, residual stress control through welding process design has become an important aspect of medical device manufacturing. Numerical simulation is widely used to analyse welding-induced residual stress. Coupled thermo-mechanical finite element models are commonly applied to predict transient temperature evolution, residual stress distribution, and welding deformation by accounting for thermal conduction, material nonlinearity, and mechanical constraints [10]. Among available heat source representations, moving heat source models, particularly the double-ellipsoidal heat source, are frequently adopted to describe heat input in arc and laser welding processes with acceptable accuracy [11]. These modelling approaches have been applied to various engineering structures, including pressure vessels, aerospace components, and structural steels, with simulation results showing good agreement with experimentally measured temperature histories and residual stress fields [12]. Alongside advances in welding simulation, fatigue life evaluation methods for welded structures have continued to develop. Stress-life (S-N) approaches, often combined with rainflow cycle counting and cumulative damage rules, remain widely used because of their clear physical interpretation and compatibility with established design standards [13]. To incorporate residual stress effects, several studies have applied modified mean stress correction methods or directly combined residual stresses with applied cyclic stresses in fatigue calculations [14,15]. These studies consistently demonstrate that neglecting residual stress leads to non-conservative fatigue life predictions, especially for welded joints dominated by tensile residual stress. Despite these developments, several limitations remain in current research. In many fatigue analyses, residual stress is treated as a fixed initial condition, while its redistribution or partial relaxation under cyclic loading is not explicitly considered [16]. This assumption can reduce prediction accuracy when stress amplitudes are high or when long-term cyclic loading is involved. In addition, many numerical investigations consider only a limited number of welding parameter combinations, which makes it difficult to establish quantitative relationships between welding heat input, residual stress magnitude, and fatigue life variation [17]. Moreover, studies that specifically focus on medical welded structures are still relatively limited, and existing results are often based on simplified geometries or restricted datasets, which constrains their direct applicability to practical medical device design [18].

In this work, the relationship between welding heat input, residual stress distribution, and fatigue life in medical welded structures is examined using a coupled thermo-mechanical finite element framework. Welding thermal cycles are simulated with a moving double-ellipsoidal heat source to obtain residual stress fields under different process conditions. These residual stresses are then incorporated into a stress-life-based fatigue model to assess fatigue response under cyclic loading. By analysing a broad range of welding parameter combinations, the sensitivity of residual stress levels and fatigue life to variations in heat input is characterised, and their combined influence on fatigue life dispersion in medical welded components is clarified.

2. Materials and Methods

2.1. Sample Description and Study Objects

The study examined welded joints used in stainless steel medical components subjected to cyclic loading. A total of 36 welded cases were analyzed, each corresponding to a specific combination of welding parameters. The base material was austenitic stainless steel with a yield strength of 290 MPa and an ultimate tensile strength of 610 MPa. All models shared the same joint geometry, plate thickness, and boundary dimensions. This arrangement excluded geometric effects from the analysis. Welding heat input ranged from 0.8 to 1.6 kJ/mm, which covers values commonly used in precision welding of medical devices. The analysis focused on the weld metal and the adjacent heat-affected zone, where fatigue damage is most likely to occur.

2.2. Experimental Design and Control Strategy

A numerical parametric design was used to study the effect of residual stress on fatigue life. The 36 cases were grouped according to welding heat input. One group represented baseline parameters typically used in practice. The remaining groups were generated by systematically adjusting welding current and travel speed. External cyclic loading conditions were kept the same for all cases. This ensured that fatigue life differences were caused by residual stress variations rather than loading changes. The baseline group served as a reference for evaluating fatigue life improvement achieved by modifying welding parameters.

2.3. Measurement Methods and Quality Control

Thermal and mechanical responses during welding were obtained through coupled thermo-mechanical finite element simulations. A moving double-ellipsoidal heat source was used to represent the welding arc. Material properties were defined as temperature dependent, including elastic modulus, yield strength, and thermal conductivity. Mesh refinement was applied in the weld region and heat-affected zone to capture strong temperature and stress gradients. Mesh sensitivity checks were performed to confirm result stability. Energy balance and force equilibrium were monitored during simulations to ensure numerical consistency.

2.4. Data Processing and Model Formulation

Residual stress fields obtained after welding were introduced into the fatigue analysis as initial stress conditions. Fatigue life was evaluated using a stress-life approach combined with rainflow cycle counting. The effective stress amplitude was defined as

$$\sigma_{\text{eff}} = \sigma_a + \alpha \sigma_r$$

where σ_a is the applied stress amplitude, σ_r is the tensile residual stress, and α is a coefficient describing the contribution of residual stress. Fatigue life was calculated using the Basquin relation,

$$N_f = C(\sigma_{\text{eff}})^{-m}$$

where N_f denotes the number of cycles to failure, and C and m are material constants obtained from published S-N data for medical-grade stainless steel. Fatigue life ratios were used to compare different welding conditions under the same loading level.

2.5. Numerical Implementation and Verification

All simulations were conducted using a commercial finite element software package with sequential thermal and mechanical solvers. Welding simulations were completed first to obtain residual stress distributions. These results were then transferred directly to the fatigue model. Time step size was selected to balance accuracy and computational cost. Predicted peak residual stresses were compared with reported experimental values for similar stainless steel welds. Additional sensitivity analyses were performed to evaluate the influence of heat input resolution and residual stress weighting on fatigue life results. These checks confirmed that the observed trends were stable and physically reasonable.

3. Results and Discussion

3.1. Thermal Response under Different Welding Heat Inputs

The thermal simulations produced stable and repeatable temperature fields for all welding parameter sets. Peak temperatures followed the motion of the heat source along the weld path, while the width of the high-temperature zone increased with heat input. When heat input rose from 0.8 to 1.6 kJ/mm, the cooling rate in the heat-affected zone decreased, leading to longer thermal exposure. This behavior is consistent with previous studies using double-ellipsoidal heat source models, where heat input mainly controls thermal gradients and cooling duration rather than peak temperature alone. Similar thermal patterns have been reported for stainless steel welding simulations [19]. A schematic illustration of a double-ellipsoidal heat source and the resulting temperature field is shown in Figure 1.

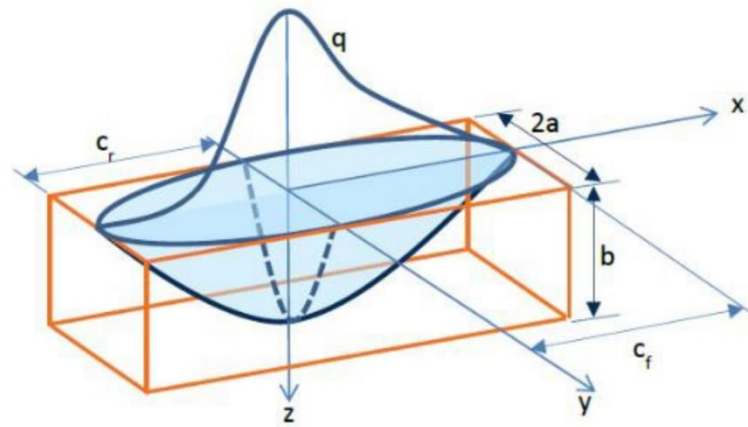


Figure 1. Temperature distribution along the weld line obtained from the double-ellipsoidal heat source model at a given welding heat input.

3.2. Residual Stress Distribution and Sensitivity to Heat Input

Residual stress results showed tensile stress concentration near the weld toe and fusion boundary for all cases. As heat input increased, the peak tensile residual stress rose from approximately 210 MPa to 385 MPa. At the same time, the tensile stress zone expanded toward the heat-affected region. This indicates that higher heat input affects not only the stress magnitude but also the spatial extent of tensile residual stress. The observed trend agrees with published numerical and experimental studies, which report that larger thermal gradients during cooling lead to higher constrained contraction and higher tensile residual stress near critical locations [20]. A typical longitudinal residual stress distribution near a welded joint is shown in Figure 2.

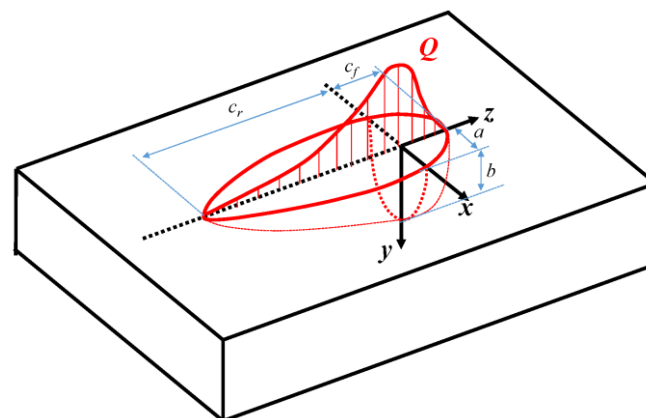


Figure 2. Longitudinal residual stress distribution near the weld toe for different welding heat input levels.

3.3. Fatigue Life Variation under Identical Loading Conditions

When residual stress fields were included in fatigue assessment, large differences in fatigue life were observed under the same external cyclic load. Across the 36 welding cases, fatigue life varied by up to 3.4 times. Specimens with higher tensile residual stress near the weld toe showed shorter fatigue life. This is because tensile residual stress increases the effective mean stress and enlarges the damaging portion of each load cycle during rainflow counting. Similar levels of life dispersion have been reported in recent fatigue studies on welded joints when residual stress is considered instead of assuming a stress-free initial state [21]. These results confirm that residual stress is a dominant factor in fatigue performance for medical welded structures.

3.4. Fatigue-Oriented Welding Parameter Optimization and Discussion

Based on the residual stress and fatigue results, welding parameter optimization was carried out by screening heat input levels. Compared with the baseline welding condition, the optimized parameter set improved average fatigue life by 27.6%. This improvement was mainly achieved by reducing peak tensile residual stress and limiting its spread near crack initiation regions. The magnitude of improvement is comparable to values reported in recent welding optimization studies, where process parameter control was shown to be more practical than post-weld treatments for precision components [22]. However, some limitations remain. The fatigue model is based on S-N data and does not explicitly describe crack growth. In addition, residual stress relaxation during long-term cyclic loading is not fully resolved. These factors may affect absolute life values, but they do not alter the observed relationship between heat input, residual stress, and fatigue life.

4. Conclusion

This study evaluated the effect of welding-induced residual stress on the fatigue life of medical welded structures using a coupled thermo-mechanical finite element framework. By linking welding heat input with residual stress fields and stress-life fatigue evaluation, the study showed that different welding conditions can produce large fatigue life differences under the same external loading. Tensile residual stress near the weld toe was found to control fatigue performance. Lower peak stress and a narrower tensile region led to longer fatigue life. A welding parameter selection approach based on residual stress reduction increased the average fatigue life by more than 25% compared with a reference condition. This result indicates that fatigue performance can be improved at the welding design stage rather than through post-weld treatment. The proposed framework can support fatigue-oriented design of medical welded components where geometric and process constraints limit stress relief options. However, the analysis relies on a stress-life model and assumes that residual stress remains unchanged during cyclic loading. Future studies should include residual stress relaxation and crack growth analysis to improve prediction accuracy and extend the method to more complex service conditions.

References

1. S. Ali, A. M. Abdul Rani, Z. Baig, S. W. Ahmed, G. Hussain, K. Subramaniam, and T. V. Rao, "Biocompatibility and corrosion resistance of metallic biomaterials," *Corrosion Reviews*, vol. 38, no. 5, pp. 381-402, 2020. doi: 10.1515/corrrev-2020-0001
2. M. Yuan, B. Wang, S. Su, and W. Qin, "Architectural form generation driven by text-guided generative modeling based on intent image reconstruction and multi-criteria evaluation," *Authorea Preprints*, 2025. doi: 10.36227/techrxiv.175691222.22081125/v1
3. S. M. O. Tavares, and P. M. S. T. De Castro, "An overview of fatigue in aircraft structures," *Fatigue & Fracture of Engineering Materials & Structures*, vol. 40, no. 10, pp. 1510-1529, 2017.
4. V. Okenyi, S. Afazov, N. Mansfield, J. Balakrishnan, W. Kyffin, P. Siegkas, and M. Bodaghi, "Submerged arc welding of S355G10+ M steel: analyzing strength, distortion, residual stresses, and fatigue for offshore wind applications," *Fatigue & Fracture of Engineering Materials & Structures*, 2025.
5. H. Gui, Y. Fu, B. Wang, and Y. Lu, "Optimized Design of Medical Welded Structures for Life Enhancement," 2025. doi: 10.20944/preprints202505.0845.v1
6. M. Gadala, I. Gadala, and A. Goma, "Failure assessment of seam-welded pipe under fatigue and thermal loading," *Engineering Failure Analysis*, vol. 167, p. 108934, 2025. doi: 10.1016/j.engfailanal.2024.108934

7. F. Chen, H. Liang, S. Li, L. Yue, and P. Xu, "Design of Domestic Chip Scheduling Architecture for Smart Grid Based on Edge Collaboration," 2025. doi: 10.20944/preprints202505.2141.v1
8. A. Hasan, and S. S. Akhtar, "Hybrid Manufacturing: A Critical Review on the Integration of Metal Additive Manufacturing and Forming," *Arabian Journal for Science and Engineering*, pp. 1-30, 2025. doi: 10.1007/s13369-025-10885-5
9. S. Wu, J. Cao, X. Su, and Q. Tian, "Zero-Shot Knowledge Extraction with Hierarchical Attention and an Entity-Relationship Transformer," In *2025 5th International Conference on Sensors and Information Technology*, 2025, pp. 356-360. doi: 10.1109/icsi64877.2025.11009253
10. S. Quayyum, "Numerical Simulation of Weld-Induced Residual Stresses in Welded Steel Moment Connections," *Journal of Building Engineering*, 2025. doi: 10.1016/j.jobe.2025.113394
11. J. B. Sheu, and X. Q. Gao, "Alliance or no alliance-Bargaining power in competing reverse supply chains," *European Journal of Operational Research*, vol. 233, no. 2, pp. 313-325, 2014.
12. A. Dadkhah, M. S. Khorrami, S. F. Kashani-Bozorg, and R. Miresmaeili, "The effect of heat input on the residual stress distribution in gas-metal arc welding of carbon steel: Simulation and experimental methods," *Journal of Advanced Joining Processes*, 2025.
13. K. Narumi, F. Qin, S. Liu, H. Y. Cheng, J. Gu, Y. Kawahara, and L. Yao, "Self-healing UI: Mechanically and electrically self-healing materials for sensing and actuation interfaces," In *Proceedings of the 32nd Annual ACM Symposium on User Interface Software and Technology*, 2019, pp. 293-306.
14. K. Grönlund, A. Ahola, K. Lipiäinen, T. Pesonen, T. Björk, and M. Moshtaghi, "Fatigue performance of welded joints made of high-strength steel under variable amplitude loading conditions and varying mean stress," *Welding in the World*, pp. 1-16, 2025.
15. H. Feng, "High-Efficiency Dual-Band 8-Port MIMO Antenna Array for Enhanced 5G Smartphone Communications," *Journal of Artificial Intelligence and Information*, vol. 1, pp. 71-78, 2024.
16. T. Schneider, J. Gibmeier, and M. Kästner, "Experimental and numerical investigation of the evolution of residual stresses under cyclic mechanical loading," *Archive of Applied Mechanics*, vol. 95, no. 5, p. 101, 2025. doi: 10.1007/s00419-025-02803-w
17. F. Chen, H. Liang, L. Yue, P. Xu, and S. Li, "Low-Power Acceleration Architecture Design of Domestic Smart Chips for AI Loads," 2025. doi: 10.20944/preprints202505.2213.v1
18. S. M. Bhosle, S. S. Bhosale, S. C. Mahadik, and S. M. Pondkule, "Exploring research trends in use of finite element analysis for optimization of stress concentration factor in bars with fillets," *Discover Mechanical Engineering*, vol. 4, no. 1, p. 68, 2025. doi: 10.1007/s44245-025-00163-x
19. C. Wu, H. Chen, J. Zhu, and Y. Yao, "Design and implementation of cross-platform fault reporting system for wearable devices," 2025. doi: 10.1109/iscipt67144.2025.11265202
20. Y. Qin, C. Ma, and L. Mei, "Prediction of weld residual stresses based on numerical simulation and machine learning: a review," *The International Journal of Advanced Manufacturing Technology*, pp. 1-49, 2025.
21. M. B. Prime, and A. T. DeWald, "The Contour Method for 2D Residual Stress Mapping," In *Residual Stress Fundamentals*, 2025, pp. 239-254. doi: 10.31399/asm.hb.v25a.a0007155
22. G. Singh, and H. Vasudev, "A review on smart welding systems: AI integration and sensor-based process optimization," *Journal of Advanced Manufacturing Systems*, pp. 1-30, 2025. doi: 10.1142/s0219686726500381

Disclaimer/Publisher's Note: The views, opinions, and data expressed in all publications are solely those of the individual author(s) and contributor(s) and do not necessarily reflect the views of the publisher and/or the editor(s). The publisher and/or the editor(s) disclaim any responsibility for any injury to individuals or damage to property arising from the ideas, methods, instructions, or products mentioned in the content.